

Extracting Classical Lyapunov Exponent from One-Dimensional Quantum Mechanics

Takeshi MORITA*

*Department of Physics, Shizuoka University,
836 Ohya, Suruga-ku, Shizuoka 422-8529, Japan
Graduate School of Science and Technology, Shizuoka University,
836 Ohya, Suruga-ku, Shizuoka 422-8529, Japan*

Abstract

Out-of-time-order correlator (OTOC) $\langle [x(t), p]^2 \rangle$ in an inverted harmonic oscillator (IHO) in one-dimensional quantum mechanics exhibits remarkable properties. The quantum Lyapunov exponent computed through the OTOC precisely agrees with the classical one. Besides, it does not show any quantum fluctuations for arbitrary states. Hence, the OTOC may be regarded as ideal indicators of the butterfly effect in the IHO. Since IHOs are ubiquitous in physics, these properties of the OTOCs might be seen in various situations too. In order to clarify this point, as a first step, we investigate the OTOCs in one dimensional quantum mechanics with polynomial potentials, which exhibit butterfly effects around the peak of the potential in classical mechanics. We find two situations in which the OTOCs show exponential growths reproducing the classical Lyapunov exponent of the peak. The first one, which is obvious, is using suitably localized states near the peak and the second one is taking a double scaling limit akin to the non-critical string theories.

arXiv:2105.09603v1 [hep-th] 20 May 2021

*E-mail address: morita.takeshi@shizuoka.ac.jp

1 Introduction

Inverted harmonic oscillators (IHOs) are ubiquitous in our nature. If we drew a random potential, we would see peaks as many as valleys. The valleys will be approximated by harmonic oscillators (HOs), and the peaks will be approximated by IHOs. Needless to say, HOs play indispensable roles in physics particularly in stable systems. Correspondingly, IHOs do the same roles in unstable systems.

Especially, IHOs appear in several important topics in modern physics: dynamical systems and chaos [1], Schwinger mechanism [2, 3, 4], non-critical string theories [5, 6, 7, 8], toy models of black holes [9, 10, 11, 12, 13, 14, 15, 16], acoustic Hawking radiation in quantum fluid mechanics [17, 18, 19, 20, 21, 22], and condensed matter systems [23, 24].

These examples show some instabilities, and they may be quantified by Lyapunov exponents at classical level. Recently, as a counterpart of this quantity in quantum mechanics, out-of-time-order correlator (OTOC) [25] defined by

$$C(t) := -\langle [W(t), V(0)]^2 \rangle, \quad (1.1)$$

draw attention [26, 27, 28]. Here, we use the Heisenberg picture, and W and V are some operators in the system, and $W(t) = e^{iHt/\hbar}W(0)e^{-iHt/\hbar}$ by using the Hamiltonian H . If we take $W = x$ and $V = p$ in a quantum mechanical system, (1.1) becomes

$$-\frac{1}{\hbar^2}\langle [x(t), p(0)]^2 \rangle \rightarrow \{x(t), p(0)\}^2 = \left(\frac{\partial x(t)}{\partial x(0)} \right)^2, \quad (1.2)$$

where we have used the classical-quantum correspondence, $[,]/i\hbar \rightarrow \{, \}$. Thus, the OTOC would evaluate the dependence of the initial condition of the time evolutions. Particularly, if the system shows the butterfly effect at the classical level, the OTOC may develop as $C(t) \sim e^{2\lambda t}$, where λ is the Lyapunov exponent. Hence, OTOCs may quantify the butterfly effects in quantum mechanics.

However, the relation between OTOCs and Lyapunov exponents are subtle. Firstly, we have assumed the classical-quantum correspondence, and it does not work generally. Secondary, even if the classical-quantum correspondence is satisfied at the early stage of the time evolution, it may break down after the Ehrenfest time and the exponential development may not be observed after that. Thus, detecting exponential developments in quantum systems would be harder than the classical ones[28]. Hence, it would be valuable to understand when we observe $C(t) \sim e^{2\lambda t}$ in order to reveal properties of OTOCs. Since IHOs also show

butterfly effects, it is natural to investigate the OTOCs in IHOs in detail, and study the application to the aforementioned various systems.

In this article, for simplicity, we consider the IHO in one-dimensional quantum mechanics [29, 30, 31, 32].

$$H = \frac{1}{2}p^2 - \frac{1}{2}\lambda^2 x^2. \quad (1.3)$$

Here, λ is the Lyapunov exponent as we will see soon. The quantum Lyapunov exponent in the IHO has been computed by evaluating an OTOC in Ref. [29], and it exactly agrees with the classical one. Particularly, the results of Ref. [29] imply the following relation,

$$\left\langle \left(\frac{1}{i\hbar} [x(t), p(0)] \right)^n \right\rangle = \cosh^n \lambda t = (\{x(t), p(0)\})^n. \quad (1.4)$$

Here, the left-hand side evaluates the OTOC in the IHO (1.3) for any normalizable quantum states and the right-hand side is the Poisson bracket for any initial conditions in classical mechanics. Since $\cosh(\lambda t) \sim e^{\lambda t}$ at a large t , this relation shows that the Lyapunov exponent of this system is λ in both classical and quantum mechanics as Ref. [29] found. Not only that this relation works for any time even after the Ehrenfest time, which is typically given by $t \sim \frac{1}{\lambda} \log \frac{1}{\hbar}$ [28]¹. Furthermore, this relation suggests that the operator $[x(t), p(0)]$ does not show any quantum fluctuations and the deviation is precisely zero. Thus, the OTOC $[x(t), p(0)]$ exhibits quite peculiar properties in the IHO, which cannot be seen regular observables, like $x(t)$ and $p(t)$. These results suggest that the OTOC $[x(t), p(0)]$ may be regarded as an ideal indicator of the butterfly effect in the IHO.

Then, it is natural to ask whether these remarkable properties of the OTOCs are held in more general situations. In order to understand this question, we study one-dimensional quantum mechanics with polynomial potentials [32, 33]. In classical mechanics, the particle motions confined in the potentials are periodic. However, if the potential has a hill, the hill will be approximated by an IHO and the system shows a butterfly effect near there. We argue when the OTOCs reproduce this classical Lyapunov exponent in quantum mechanics. As is expected through the classical-quantum correspondence, we will see that suitably localized wave packets correctly reproduce the Lyapunov exponent. Besides, if we take a double scaling limit similar to the non-critical string theories [5, 6, 7, 8], the correct Lyapunov exponent will be obtained through more general states such as energy eigenstates.

¹The Ehrenfest time $t \sim \frac{1}{\lambda} \log \frac{1}{\hbar}$ is estimated as the time scale that a wave packet spreads over the curvature scale of the IHO. However, the domain of the IHO (1.3) is infinite ($-\infty \leq x \leq \infty$), and it may be reasonable that the naive Ehrenfest time does not work in our case.

2 No Quantum Fluctuation of the OTOCs in the IHO

We prove the relation (1.4). We start from classical mechanics. The classical solution of the Hamiltonian (1.3) is given by

$$x(t) = x(0) \cosh \lambda t + \frac{1}{\lambda} p(0) \sinh \lambda t, \quad (2.1)$$

where $x(0)$ and $p(0)$ are the initial conditions of the position $x(t)$ and momentum $p(t)$. Then, we can compute the Poisson bracket as

$$\{x(t), p(0)\} = \frac{\partial x(t)}{\partial x(0)} = \cosh \lambda t, \quad (2.2)$$

and the second equality in the relation (1.4) is satisfied.

Next, we consider quantum mechanics. As Ref. [29, 31] pointed out, we obtain

$$x(t) = e^{iHt} x(0) e^{-iHt} = x(0) \cosh \lambda t + \frac{1}{\lambda} p(0) \sinh \lambda t, \quad (2.3)$$

through the the Hadamard lemma, and it leads to

$$[x(t), p(0)] = i\hbar \cosh \lambda t. \quad (2.4)$$

Since this quantity is a c-number, the relation (1.4) is satisfied for any normalizable states. Obviously, similar relations will be held for other OTOC $[p(t), p(0)]$, $[x(t), x(0)]$ and $[p(t), x(0)]$.

However, the result (1.4) is subtle, since the IHO potential (1.3) is unbounded from below and the energy eigen-functions of the IHO (1.3) are not normalizable. Hence it would be valuable to test the relation (1.4) explicitly. We add the infinite potential walls at $x = \pm\Lambda$ to the IHO (1.3) to make the system bounded, and compute the OTOC $\langle [x(t), p(0)] \rangle$ and $\langle [x(t), p(0)]^2 \rangle$ for several Gaussian wave packets numerically². We find very good agreement between classical and quantum mechanics as shown in FIG.1, and the quantum fluctuations of the operator $[x(t), p(0)]$ are indeed almost zero.

Note that, if we replace λ with $i\omega$, ($\omega \in \mathbf{R}$) in the Hamiltonian (1.3), we obtain a similar relation for the harmonic oscillator (HO),

$$\left\langle \left(\frac{1}{i\hbar} [x(t), p(0)] \right)^n \right\rangle = \cos^n \omega t = (\{x(t), p(0)\})^n. \quad (2.5)$$

Actually, we can derive this relation directly from the relation $\langle m | [x(t), p(0)] | n \rangle = i\hbar \delta_{mn} \cos \omega t$, which we can easily obtain by solving the HO through the standard method [34].

²We use Mathematica package NDEigensystem in the numerical calculations. However, this package sometimes fails to obtain eigen-functions that have suitable parity symmetry $x \rightarrow -x$. Hence, we take the domain $0 \leq x \leq \Lambda$ rather than $-\Lambda \leq x \leq \Lambda$, and solve the even and odd solutions separately by imposing the corresponding boundary conditions at $x = 0$.

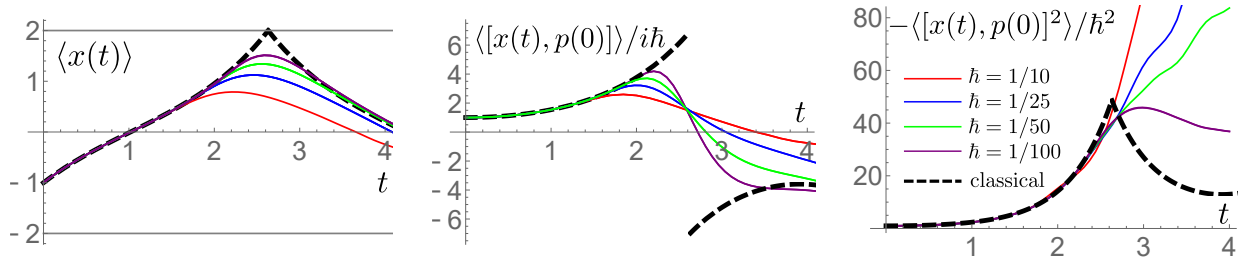


Figure 1: Time evolutions of $x(t)$ and the OTOCs in the IHO (1.3). We take $\lambda = 1$ and put the infinite potential walls at $x = \pm 2$. We prepare the Gaussian wave packets with $(\Delta x)^2 = (\Delta p)^2$ centered at $(x, p) = (-1, 1.3)$ at $t = 0$, and evaluate their time evolutions in the quantum mechanics with $\hbar = 1/10, 1/25, 1/50$ and $1/100$. We also compute the corresponding quantities for a single classical particle, which are depicted by the black dashed lines. $\langle x(t) \rangle$ shows that the wave packets hit the potential wall at $x = 2$ around $t \sim 2.5$. All the OTOCs agree very well until the hits, and they are independent of \hbar . Thus, the relation (1.4) works as far as we can ignore the effect of the potential walls.

3 OTOCs in General Potentials

So far, we have seen that the quantum fluctuations of the OTOCs in the IHO and HO are exactly zero. This is because $x(t)$ (2.1) is linear in $x(0)$ and $p(0)$, and it will not happen in general potential $V(x)$. On the other hand, if the potential $V(x)$ has a hill (valley), the region near the hill (valley) will be approximated by the IHO (HO) and the quantum fluctuations of the OTOCs will be suppressed. Particularly, a classical particle near the hill will show a butterfly effect, and the Lyapunov exponent is computed from the curvature of the potential as

$$\lambda_{\text{saddle}} := \sqrt{V'(x)} \Big|_{x=x_{\text{saddle}}} . \quad (3.1)$$

Here, we have taken $x = x_{\text{saddle}}$ as the position of the top of the hill, since it is a saddle point in the phase space and we have defined λ_{saddle} as the Lyapunov exponent associated with this point. Hence, if we can prepare sufficiently localized wave packets corresponding to classical particles near the hill, the OTOCs would show the exponential developments with the Lyapunov exponent λ_{saddle} and the quantum corrections would be small. (In order to prepare such localized wave packets in general potential $V(x)$, the potential hill should be sufficiently isolated.) Indeed, we have seen in FIG. 1 that the deformation of the IHO potential by the infinite walls do not affect the relation (1.4).

Then, one question is whether one can obtain λ_{saddle} through the OTOCs without using the localized wave packets. Particularly, energy eigenstates compose the basis of the Hilbert

space, and it is natural to try to evaluate the OTOCs for these states. However, energy eigenstates generally do not represent a localized particle in the position space, and obtaining λ_{saddle} from them seems non-trivial. In order to test it, we numerically evaluate the OTOC $\langle [x(t), p(0)] \rangle$ and $\langle [x(t), p(0)]^2 \rangle$ for the energy eigenstates in the potential³ $V(x) = -ax^2 + bx^4$ and $V(x) = -ax^2 + bx^8$, ($a, b > 0$). The results are summarized in FIG.2. We do not observe clear exponential developments for $\langle [x(t), p(0)] \rangle$. On the other hand, exponential growths are observed for $\langle [x(t), p(0)]^2 \rangle$, but the exponents depend on the shape of the potentials. Although the exponent in the $V(x) = -ax^2 + bx^8$ case is close to $2\lambda_{\text{saddle}}$, it is significantly smaller in the $V(x) = -ax^2 + bx^4$ case⁴. Besides, the results must depend on the energy level. For example, if the energy is close to the ground state, the particles are localized near the bottom of the potential, and we would observe the cos type behaviors as in (2.5) rather than exponential developments.

Actually, if we tune the energy level and \hbar such that

$$E \rightarrow E_{\text{cr}} := V(x_{\text{saddle}}), \quad \hbar \rightarrow 0, \quad (3.2)$$

the OTOCs for the energy eigenstate show the exponential developments. See FIG. 3. We observe that both of the OTOC $\langle [x(t), p(0)] \rangle$ and $\langle [x(t), p(0)]^2 \rangle$ show the exponential growths with the Lyapunov exponent λ_{saddle} as we take $\hbar \rightarrow 0$. This limit is analogous to the double-scaling limit in the non-critical string theories [5, 6, 7, 8], and we call this energy as the critical energy.

This result can be explained as follows. In the WKB approximation, the probability density of the energy eigen-function ρ is proportional to the inverse of the classical momentum, $\rho \propto 1/|p|$. At $E = E_{\text{cr}} = V(x_{\text{saddle}})$, the momentum near $x = x_{\text{saddle}}$ satisfies

$$0 \sim \frac{1}{2}p^2 - \frac{1}{2}\lambda_{\text{saddle}}^2(x - x_{\text{saddle}})^2, \quad (3.3)$$

³We have attempted to evaluate the OTOCs of the energy eigenstates in the IHO with the infinite potential walls, which we have used in the numerical study of the wave packets in FIG. 1. However, we found that the convergences of numerical computations were not good and could not obtain reliable results. We presume that the infinite potential walls are problematic. Actually, if we evaluate $\{x(t), p(0)\}^2$ of a classical particle in a infinite potential well (without IHO potential) and take an average over the initial position so that it corresponds to the semi-classical energy eigenstate, we easily see that $\{x(t), p(0)\}^2$ diverges. This divergence will be resolved in quantum mechanics, but it may cause larger numerical errors.

⁴In the $V(x) = -ax^2 + bx^4$ case, the exponential development of $\langle [x(t), p(0)]^2 \rangle$ is roughly $\langle [x(t), p(0)]^2 \rangle \sim \exp(\lambda_{\text{saddle}}t) \neq \exp(2\lambda_{\text{saddle}}t)$. Similar behaviors have been observed in other models too[30], and Ref. [30] argued that the OTOCs may be suppressed by $\exp(-\lambda_{\text{saddle}}t)$ in thermal ensembles.

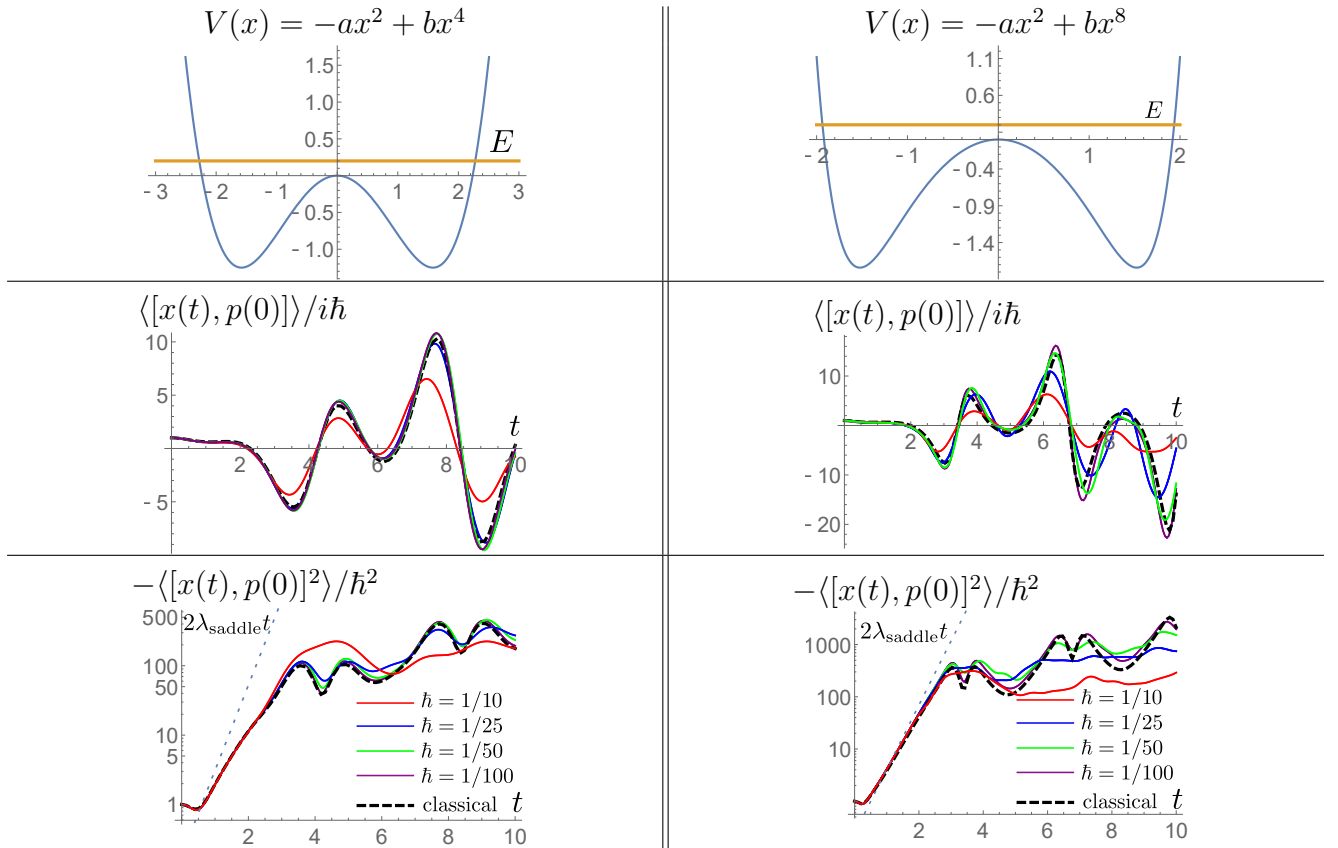


Figure 2: OTOCs for energy eigenstates in $V(x) = -ax^2 + bx^4$ ($a = 1, b = 0.2$) [LEFT] and $V(x) = -ax^2 + bx^8$ ($a = 1, b = 0.02$) [RIGHT]. The energies are taken to be $E = 0.2$ in the both cases. We evaluate $\langle [x(t), p(0)] \rangle$ and $\langle [x(t), p(0)]^2 \rangle$, and their classical counterparts, which are depicted by the black dashed lines. As $\hbar \rightarrow 0$, the OTOCs converge to the classical results. We do not observe clear exponential developments in $\langle [x(t), p(0)] \rangle$. On the other hand, we observe exponential growths in $\langle [x(t), p(0)]^2 \rangle$, but the exponent in the $V(x) = -ax^2 + bx^4$ case is significantly smaller than $2\lambda_{\text{saddle}}$, while it is close to $2\lambda_{\text{saddle}}$ in the $V(x) = -ax^2 + bx^8$ case.

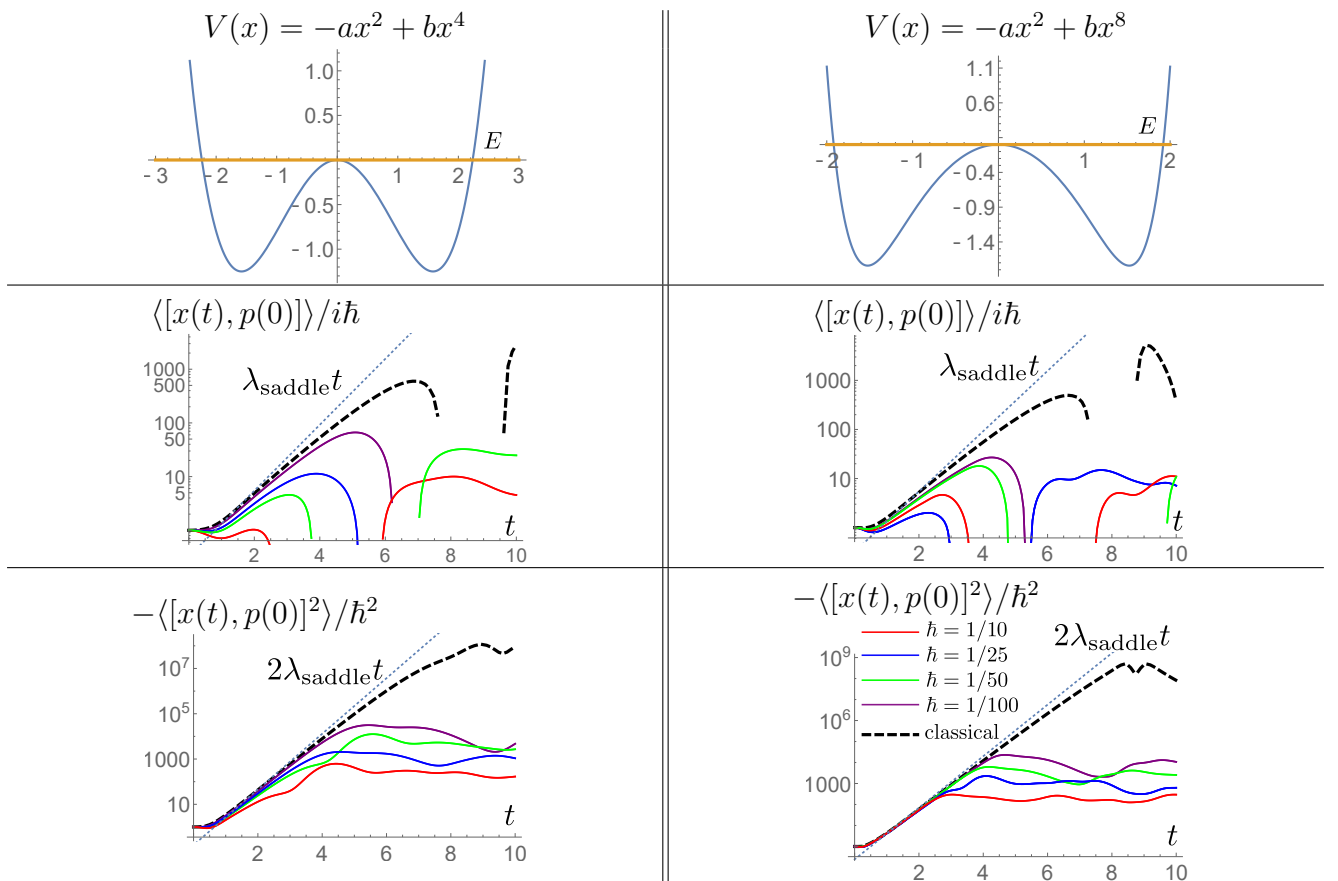


Figure 3: OTOCs at the critical energy $E = E_{\text{cr}}$ (3.2). We employed the same data to FIG. 2 except the energies. In quantum mechanics, since we cannot take $E = E_{\text{cr}}$ exactly, we choose the closest one with $E - E_{\text{cr}} > 0$, and we take $E = 0.0001$ in classical mechanics, correspondingly. We observe that all OTOCs show the exponential growths with the Lyapunov exponent λ_{saddle} as $\hbar \rightarrow 0$, and the relation (1.4) are approximately satisfied.

and the density ρ shows a divergence

$$\rho \propto \frac{1}{|p|} \propto \frac{1}{|x - x_{\text{saddle}}|}. \quad (3.4)$$

Therefore, when we evaluate observables, the contribution of the saddle points would dominate⁵. However, quantum corrections make this divergence milder. By combining these two effects, the OTOCs exhibit the behaviors similar to the IHO near the saddle point as $E \rightarrow E_{\text{cr}}$ and $\hbar \rightarrow 0$. Note that, if we prepare some states that are constructed from energy eigenstates whose energies are close to E_{cl} , their OTOCs may also show the exponential growths.

Finally, we comment on the classical limit. As we can see in FIG.2 and FIG.3, the OTOCs converge to the classical results as $\hbar \rightarrow 0$. Thus, we can explain the behaviors of the OTOCs through classical mechanics. In Appendix, we will discuss the following two questions: (1) Why are the exponents in FIG.2 and FIG.3 always smaller than λ_{saddle} or $2\lambda_{\text{saddle}}$. (2) Why does $\langle [x(t), p(0)]^2 \rangle$ show the exponential development while $\langle [x(t), p(0)] \rangle$ does not in FIG.2.

4 Discussions

We have studied the OTOC $\langle [x(t), p(0)]^n \rangle$ in the IHO. They show a peculiar property that they do not show any quantum fluctuations independent of the quantum states. This suggests that the OTOCs can be regarded as ideal indicators of the butterfly effect in the IHO. Hence, we expect that the IHO may work as a starting point of perturbative calculations in unstable systems and chaos, and the Lyapunov exponents of the systems may be extracted through the OTOCs. (The situation may be analogous to HOs in stable systems.) Indeed, we have seen that we can derive the Lyapunov exponents of the saddle points by preparing sufficiently localized wave packets or by employing the double scaling limit $E \rightarrow E_{\text{cr}}$ and $\hbar \rightarrow 0$ in one-dimensional quantum mechanics. However, one-dimensional system is integrable and it would be important to apply our results to more complicated systems or genuine chaotic systems. (See [30, 31, 32, 33, 34, 35, 36, 37, 38, 39, 40, 41, 42] and references therein for investigations of OTOCs in few-body quantum mechanics.)

Besides, as we mentioned in the introduction, IHOs have a wide range of applications from condensed matter systems to quantum gravities. Thus, it is interesting to study the

⁵The momentum becomes zero at the turning point $x = x_*$ also, at which $E = V(x_*)$ is satisfied. However, the momentum normally behaves as $|p| \sim (x - x_*)^{1/2}$, and the divergence is much milder than that of the saddle point at the critical energy (3.4). Hence, the turning points do not provide dominate contributions.

implications that the OTOCs do not receive any quantum corrections in these systems.

Acknowledgements The author would like to thank Koji Hashimoto for valuable discussions and comments. A part of numerical computation in this work was carried out at the Yukawa Institute Computer Facility. The work of T. M. is supported in part by Grant-in-Aid for Scientific Research C (No. 20K03946) from JSPS.

A Reproducing the OTOCs from Classical Mechanics

In this appendix, we argue the derivation of the Poisson bracket $\{x(t), p(0)\}^n$ that is the counterpart of the OTOC $\langle [x(t), p(0)]^n \rangle$ in classical mechanics. By using it, we will understand the time evolutions of the OTOCs in FIG. 2 and 3 from the view point of classical mechanics.

In classical mechanics, the energy eigenstate in quantum mechanics can be approximated by using the particles uniformly distributed on the constant energy curve in the phase space. See FIG.4. Then, physical quantities for the energy eigenstate can be computed by taking the averages of the quantities for each particle. Hence, to obtain the OTOC, we need to compute $\{x(t), p(0)\}^n$ for single particles and take the average of them.

First we consider the Poisson bracket $\{x(t), p(0)\}$ for a single particle. Suppose that a particle starts from $(x, p) = (x(0), p(0))$ at $t = 0$, and we define the position of this particle at time t as $x(t, x(0), p(0))$. Then, we can compute

$$\{x(t), p(0)\} = \frac{\partial x(t)}{\partial x(0)} = \lim_{\Delta x \rightarrow 0} \frac{x(t, x(0) + \Delta x, p(0)) - x(t, x(0), p(0))}{\Delta x}. \quad (\text{A.1})$$

To evaluate the right-hand side of this equation, we need to compute the positions of the two particle $x(t, x(0) + \Delta x, p(0))$ and $x(t, x(0), p(0))$. See FIG.4. Generally, we cannot obtain the particle positions explicitly, and we evaluate them numerically and extrapolate the limit $\Delta x \rightarrow 0$.

Let us consider the motions of the two particles in (A.1) in the potential $V(x) = -ax^2 + bx^4$. Each particle periodically moves in the phase space. The period depends on the energy of the particle, and it becomes longer as $E \rightarrow E_{\text{cr}}$. (Actually, it diverges at $E = E_{\text{cr}}$, and its motion is not periodic anymore.) Thus, for example, in the case of the two particles plotted in FIG.4, the period of the left particle is longer, and, when the left particle returns to its original position, the right particle moves slightly ahead of its original position. Hence,

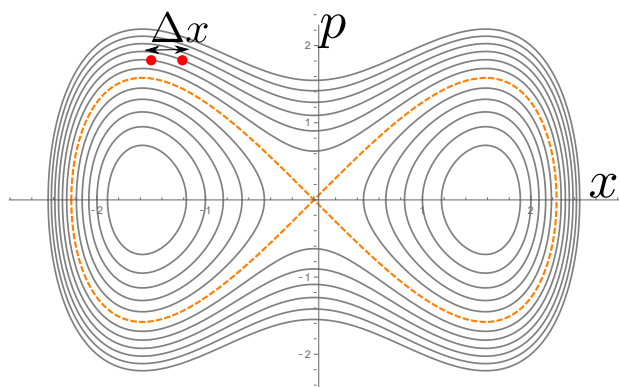


Figure 4: Constant energy curves (energy contours) in the phase space for the potential $V(x) = -ax^2 + bx^4$, ($a > 0$, $b > 0$). The orange dashed line denotes the critical energy E_{cr} . We can compute the Poisson bracket (A.1) by evaluating the motions of the two particles separated by Δx at $t = 0$. Each particle orbits in a clockwise direction along the constant energy curve, and the Poisson bracket (A.1) can be obtained through the deviation of the positions of these particles.

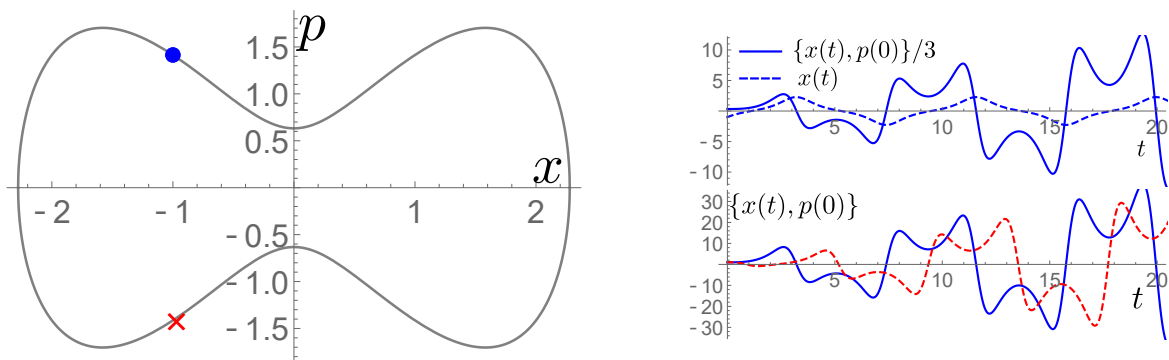


Figure 5: $\{x(t), p(0)\}$ for two classical particles in the potential $V(x) = -ax^2 + bx^4$ with a common energy ($E = 0.2$). (LEFT) The two particles in the phase space at $t = 0$. The solid line denotes the constant energy curve. (RIGHT TOP) The particle position $x(t)$ (blue dashed line) and $\{x(t), p(0)\}$ (blue solid line) for the blue dot particle in the left panel. $x(t)$ shows a periodic motion with a period $T \simeq 8.4$. Correspondingly, $\{x(t), p(0)\}$ is roughly periodic but progressively increases. It shows the exponential development when $x(t)$ passes 0, which is the position of the potential hill, and takes the maximum value before the turning point ($x \simeq 2.3$), and suddenly decreases around the turning point. (RIGHT BOTTOM) $\{x(t), p(0)\}$ for the blue dot particle (the blue line) and for the red cross one (the red dashed line) in the left panel.

$\{x(t), p(0)\}$ is almost periodic but progressively increases for each period. See FIG. 5. In addition, since the two particle motions are almost periodic, $\{x(t), p(0)\}$ has to be zero at least twice for each period, and the sign of $\{x(t), p(0)\}$ changes when it crosses these zero points. (Otherwise, the two particles could not return to their original positions.) In the case of the HO (2.5), $t = \pi/2\omega$ and $3\pi/2\omega$ correspond to the zero points.

Besides, when the particles pass near the hill of the potential, they show exponential growths similar to (2.1), and $\{x(t), p(0)\}$ also develops exponentially. On the other hand, when the particles move in the potential valleys, their motions are like oscillators and $\{x(t), p(0)\}$ will show a cos type behavior similar to (2.5). In this way, we can roughly explain the time evolution of $\{x(t), p(0)\}$ in FIG. 5.

So far, we have discussed the properties of $\{x(t), p(0)\}$ for a single particle. Now, we argue the $\{x(t), p(0)\}$ for the energy eigenstate by considering to take an average of these single particle results, and we will explain the behaviors shown in FIG. 2 in quantum mechanics. We first discuss why the Lyapunov exponents are smaller than λ_{saddle} . When we take the average, the maximum of $\{x(t), p(0)\}$ would dominate. As we can see in FIG. 5, the maximum appears after the exponential developments terminate, and, there, the growths are much slow. Hence, the Lyapunov exponents of the energy eigenstates are always smaller than λ_{saddle} .

Next we discuss why we do not observe clear exponential developments in $\langle [x(t), p(0)] \rangle$. This is because $\{x(t), p(0)\}$ for single particles take positive and negative values and they may cancel out each other when we take the average. This is very different from the OTOC $\langle [x(t), p(0)] \rangle$ for the wave packets where we have seen clear exponential developments as in FIG. 1. On the other hand, at the critical energy $E = E_{\text{cr}}$, the particles near the saddle points dominate, and such cancellation are suppressed. Hence, we observe the exponential growths as in FIG. 3.

References

- [1] S. Wiggins, *Introduction to applied nonlinear dynamical systems and chaos*. Texts Appl. Math. Springer, New York, NY, 1990.
- [2] N. Balazs and A. Voros, *Wigner's function and tunneling*, *Annals of Physics* **199** (1990), no. 1 123–140.
- [3] R. Parentani and R. Brout, *Vacuum instability and black hole evaporation*, *Nuclear Physics B* **388** (1992), no. 2 474–508.

- [4] R. Brout, S. Massar, R. Parentani, and P. Spindel, *A Primer for black hole quantum physics*, *Phys. Rept.* **260** (1995) 329–454, [[arXiv:0710.4345](#)].
- [5] I. R. Klebanov, *String theory in two-dimensions*, in *Spring School on String Theory and Quantum Gravity (to be followed by Workshop) Trieste, Italy, April 15-23, 1991*, pp. 30–101, 1991. [hep-th/9108019](#).
- [6] P. H. Ginsparg and G. W. Moore, *Lectures on 2-D gravity and 2-D string theory*, in *Theoretical Advanced Study Institute (TASI 92): From Black Holes and Strings to Particles Boulder, Colorado, June 3-28, 1992*, pp. 277–469, 1993. [hep-th/9304011](#). [[277\(1993\)](#)].
- [7] J. Polchinski, *What is string theory?*, in *NATO Advanced Study Institute: Les Houches Summer School, Session 62: Fluctuating Geometries in Statistical Mechanics and Field Theory Les Houches, France, August 2-September 9, 1994*, 1994. [hep-th/9411028](#).
- [8] Y. Nakayama, *Liouville field theory: A Decade after the revolution*, *Int. J. Mod. Phys. A* **19** (2004) 2771–2930, [[hep-th/0402009](#)].
- [9] J. L. Karczmarek, J. M. Maldacena, and A. Strominger, *Black hole non-formation in the matrix model*, *JHEP* **01** (2006) 039, [[hep-th/0411174](#)].
- [10] T. Banks, *Holographic Space-time Models in 1 + 1 Dimensions*, [arXiv:1506.05777](#).
- [11] K. Hashimoto and N. Tanahashi, *Universality in Chaos of Particle Motion near Black Hole Horizon*, *Phys. Rev.* **D95** (2017), no. 2 024007, [[arXiv:1610.06070](#)].
- [12] P. Betzios, N. Gaddam, and O. Papadoulaki, *The Black Hole S-Matrix from Quantum Mechanics*, *JHEP* **11** (2016) 131, [[arXiv:1607.07885](#)].
- [13] M. Maitra, D. Maity, and B. R. Majhi, *Near horizon symmetries, emergence of Goldstone modes and thermality*, *Eur. Phys. J. Plus* **135** (2020), no. 6 483, [[arXiv:1906.04489](#)].
- [14] S. Dalui, B. R. Majhi, and P. Mishra, *Horizon induces instability locally and creates quantum thermality*, *Phys. Rev. D* **102** (2020), no. 4 044006, [[arXiv:1910.07989](#)].
- [15] S. Dalui and B. R. Majhi, *Near horizon local instability and quantum thermality*, [arXiv:2007.14312](#).
- [16] B. R. Majhi, *Is eigenstate thermalization hypothesis the key for thermalization of horizon?*, [arXiv:2101.04458](#).
- [17] S. Giovanazzi, *Hawking radiation in sonic black holes*, *Phys. Rev. Lett.* **94** (2005) 061302, [[physics/0411064](#)].
- [18] S. Giovanazzi, *The Sonic analogue of black hole radiation*, *J. Phys.* **B39** (2006) 109, [[cond-mat/0604541](#)].

- [19] A. Parola, M. Tettamanti, and S. L. Cacciatori, *Analogue Hawking radiation in an exactly solvable model of BEC*, *EPL* **119** (2017), no. 5 50002, [arXiv:1703.05041].
- [20] T. Morita, *Semi-classical bound on Lyapunov exponent and acoustic Hawking radiation in $c = 1$ matrix model*, arXiv:1801.00967.
- [21] T. Morita, *Thermal Emission from Semi-classical Dynamical Systems*, *Phys. Rev. Lett.* **122** (2019), no. 10 101603, [arXiv:1902.06940].
- [22] T. Morita, *Analogous Hawking Radiation in Butterfly Effect*, in *4th International Conference on Holography, String Theory and Discrete Approach in Hanoi, Vietnam*, 1, 2021. arXiv:2101.02435.
- [23] S. S. Hegde, V. Subramanyan, B. Bradlyn, and S. Vishveshwara, *Quasinormal modes and the hawking-unruh effect in quantum hall systems: Lessons from black hole phenomena*, *Phys. Rev. Lett.* **123** (Oct, 2019) 156802.
- [24] V. Subramanyan, S. S. Hegde, S. Vishveshwara, and B. Bradlyn, *Physics of the Inverted Harmonic Oscillator: From the lowest Landau level to event horizons*, arXiv:2012.09875.
- [25] A. I. Larkin and Y. N. Ovchinnikov, *Quasiclassical Method in the Theory of Superconductivity*, *Soviet Journal of Experimental and Theoretical Physics* **28** (June, 1969) 1200.
- [26] Kitaev, *A simple model of quantum holography, KITP strings seminar and Entanglement 2015 program (Feb. 12, April 7, and May 27, 2015)* (2015).
- [27] Kitaev, *Hidden Correlations in the Hawking Radiation and Thermal Noise, Talk at KITP (Feb. 12, 2015)* (2015).
- [28] J. Maldacena, S. H. Shenker, and D. Stanford, *A bound on chaos*, *JHEP* **08** (2016) 106, [arXiv:1503.01409].
- [29] K. Hashimoto, K. Murata, and K. Yoshida, *Chaos in chiral condensates in gauge theories*, *Phys. Rev. Lett.* **117** (2016), no. 23 231602, [arXiv:1605.08124].
- [30] T. Xu, T. Scaffidi, and X. Cao, *Does scrambling equal chaos?*, *Phys. Rev. Lett.* **124** (2020), no. 14 140602, [arXiv:1912.11063].
- [31] A. Bhattacharyya, W. Chemissany, S. S. Haque, J. Murugan, and B. Yan, *The Multi-faceted Inverted Harmonic Oscillator: Chaos and Complexity*, *SciPost Phys. Core* **4** (2021) 002, [arXiv:2007.01232].
- [32] K. Hashimoto, K.-B. Huh, K.-Y. Kim, and R. Watanabe, *Exponential growth of out-of-time-order correlator without chaos: inverted harmonic oscillator*, *JHEP* **11** (2020) 068, [arXiv:2007.04746].
- [33] P. Romatschke, *Quantum Mechanical Out-Of-Time-Ordered-Correlators for the Anharmonic (Quartic) Oscillator*, *JHEP* **01** (2021) 030, [arXiv:2008.06056].

- [34] K. Hashimoto, K. Murata, and R. Yoshii, *Out-of-time-order correlators in quantum mechanics*, *JHEP* **10** (2017) 138, [[arXiv:1703.09435](#)].
- [35] E. B. Rozenbaum, S. Ganeshan, and V. Galitski, *Lyapunov Exponent and Out-of-Time-Ordered Correlator's Growth Rate in a Chaotic System*, *Phys. Rev. Lett.* **118** (2017), no. 8 086801, [[arXiv:1609.01707](#)].
- [36] E. B. Rozenbaum, S. Ganeshan, and V. Galitski, *Universal level statistics of the out-of-time-ordered operator*, *Phys. Rev. B* **100** (2019), no. 3 035112, [[arXiv:1801.10591](#)].
- [37] J. Chávez-Carlos, B. López-Del-Carpio, M. A. Bastarrachea-Magnani, P. Stránský, S. Lerma-Hernández, L. F. Santos, and J. G. Hirsch, *Quantum and Classical Lyapunov Exponents in Atom-Field Interaction Systems*, *Phys. Rev. Lett.* **122** (2019), no. 2 024101, [[arXiv:1807.10292](#)].
- [38] Q. Zhuang, T. Schuster, B. Yoshida, and N. Y. Yao, *Scrambling and Complexity in Phase Space*, *Phys. Rev. A* **99** (2019), no. 6 062334, [[arXiv:1902.04076](#)].
- [39] R. Prakash and A. Lakshminarayan, *Scrambling in strongly chaotic weakly coupled bipartite systems: Universality beyond the Ehrenfest timescale*, *Phys. Rev. B* **101** (2020), no. 12 121108, [[arXiv:1904.06482](#)].
- [40] R. Prakash and A. Lakshminarayan, *Out-of-time-order correlators in bipartite nonintegrable systems*, *Acta Phys. Polon. A* **136** (2019) 803–810, [[arXiv:1911.02829](#)].
- [41] T. Akutagawa, K. Hashimoto, T. Sasaki, and R. Watanabe, *Out-of-time-order correlator in coupled harmonic oscillators*, *JHEP* **08** (2020) 013, [[arXiv:2004.04381](#)].
- [42] R. A. Kidd, A. Safavi-Naini, and J. F. Corney, *Saddle-point scrambling without thermalization*, *Phys. Rev. A* **103** (2021), no. 3 033304, [[arXiv:2010.08093](#)].